

## Samarium doped boron nitride nanotubes



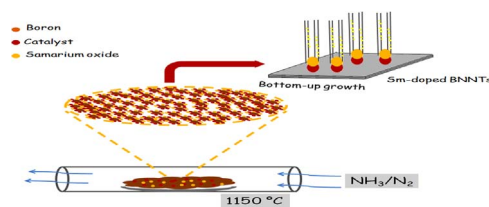
Wellington Marcos da Silva, Tiago Hilário Ferreira, Carlos Antônio de Moraes, Alexandre Soares Leal, Edésia Martins Barros Sousa\*

Nuclear Technology Development Center (CDTN) – Avenida Presidente Antônio Carlos, 6627 Pampulha, 31270-901 Belo Horizonte, MG, Brazil

### HIGHLIGHTS

- BNNTs doped in situ with samarium were synthesized by thermal chemical vapor deposition.
- Sm-doped BNNTs sample was activated by neutron capture, producing  $^{152}\text{Sm}$  radioisotopes.
- The results demonstrate that this material has great potential as a nano-system in nuclear medicine.

### GRAPHICAL ABSTRACT



### ARTICLE INFO

#### Keywords:

Boron nitride nanotubes  
Samarium  
Doping  
Synthesis  
Catalyst

### ABSTRACT

Boron nitride nanotubes doped in situ with samarium (Sm-doped BNNTs) were synthesized at 1150 °C under atmosphere of  $\text{NH}_3/\text{N}_2$  gas mixture by thermal chemical vapor deposition (TCVD) using samarium oxide that is a product of the process separation of thorium and uranium tailings. The samarium in the BNNTs sample was activated by neutron capture, in a nuclear reactor, producing  $^{152}\text{Sm}$  radioisotopes. The STEM-EELS spectrum and neutron activation show energies attributed to the samarium confirming the in situ doping process during BNNTs growth. The results demonstrate that this material has great potential as a nanosized  $\beta^-$  emission source for medical therapy.

### 1. Introduction

The synthesis of boron nitride nanotubes (BNNTs) was first reported in 1995 by Chopra, based on an arc discharge method, producing a type of one-dimensional (1D) nanostructure (Chopra et al., 1995). Currently, several methods of synthesis have been employed, such as laser ablation, autoclaving, ball milling and chemical vapor deposition (CVD). CVD is the most advanced and convenient technique for the synthesis of BNNTs because it requires a simple apparatus (Ahmad et al., 2015). Various types of catalysts may also be used in the synthesis process, including metallic oxide nanoparticles (Ferreira et al., 2011; Huang et al., 2011; Tang et al., 2002a; Koi et al., 2008; Lee et al., 2010; Matveev et al., 2015; özmen et al., 2013; Tang et al., 2002b; Wang et al., 2016). Recently BNNTs have attracted significant interest for scientific and technological applications due to their high resistance to oxidation, high thermal stability, excellent thermal conductivity, high

Young's modulus, piezoelectricity, and the ability to suppress thermal neutron radiation (Chen et al., 2004; Cohen et al., 2010; Golberg et al., 2010; Nakhmanson et al., 2003). Doping modifications can effectively tune the BNNTs electronic structure and expand their applications (Chen et al., 2010, 2008, 2007). In this sense they are a highly promising material for applications such as shields/capsules, filler for composites, self-cleaning materials, and in biology and medicine (Ciofani et al., 2013a, 2009; Golberg et al., 2010; Pakdel et al., 2011). Nanometer-sized luminescent materials are very important for potential nanometer-sized light sources, lasers, display devices and medical diagnosis (Chen et al., 2008, 2007). Wide-bandgap semiconductors doped with rare-earth ions are considered as a new type of luminescent material, combining special wide-bandgap semiconducting properties with the rare-earth luminescence feature (Liu et al., 2002; Vetter et al., 2004). BNNTs have a stable wide bandgap of 5.5 eV which makes BNNTs an ideal nanosized luminescent material (Blase et al., 1994;

\* Corresponding author.

E-mail address: [sousaem@cdtn.br](mailto:sousaem@cdtn.br) (E.M. Barros Sousa).

Museur and Kanaev, 2009). BNNTs doped with rare-earth elements with short half-life, like  $^{152}\text{Sm}$ , for example, can be used as imaging marker and for internal radiotherapy of bone metastases because, when subjected to thermal neutron flux, the radioactive isotope  $^{153}\text{Sm}$  decays with half-life of 46.3 h, emitting preferably beta-particles, turning into the stable element  $^{153}\text{Eu}$  (Qaim, 2016).

In this sense, nanomaterials have come to contributed traditional medicine with the introduction of new concepts and methods. In the and cancer diagnostics, for example, some imaging techniques, such as magnetic resonance imaging (MRI), X-ray computed tomography (CT), positron emission tomography (PET) and optical imaging are powerful tools. As for therapy methods, photodynamic therapy (PDT), photothermal therapy (PTT), delivery of chemotherapeutical drugs and techniques based on magnetism have been applied (Beckert et al., 2016; Gai et al., 2014). Following this direction, nanomaterials with specific functionalities can be used as nanovectors for delivery of proteins, drugs or genes in cancer therapy (Ciofani and Mattoli, 2016; Soares et al., 2012). On the other hand, rare-earth doped nanoparticles, which have low cytotoxicity are excellent candidates as contrast agents (Sheng et al., 2017). The use of lanthanides as radionuclides in nuclear medicine is well-known, because they can be used for detecting and treating cancerous tumors (Ascencio et al., 2005). Samarium ( $^{153}\text{Sm}$ ) Lexidronam had a combination of biologic properties necessary for a bone-targeted radiotherapeutic agent, and therefore was currently approved for the treatment of bone pain (Sartor, 2004). The use of BNNTs as a target agent of  $^{153}\text{Sm}$  can improve the efficiency of this radionuclide in the proposed therapy.

In this study, the in situ doping process of BNNTs with samarium (Sm) during growth was accomplished by the thermal chemical vapor deposition (TCVD) process. The catalyst was synthesized from an iron (III) oxalate hexahydrate and sodium borohydride mixture in our laboratory. In the next step, BNNTs with samarium were evaluated for neutron activation in a nuclear reactor. Thus, the great innovation of this work is the production of samarium-doped BNNTs by TCVD technique from samarium oxide that is a product of the separation process of thorium and uranium tailings. The results demonstrate that this material has great potential as a nanosized  $\beta^-$  emission source for medical therapy.

## 2. Experimental section

Iron (III) oxalate hexahydrate 99.9%  $\text{Fe}_2(\text{C}_2\text{O}_4)_3$ , sodium borohydride 98% ( $\text{NaBH}_4$ ) and amorphous boron powder were obtained from Sigma Aldrich and were used as received. Samarium oxide is a product of the separation process of thorium and uranium tailings. The separation and purification of rare-earth elements was made by solvent extraction method. The results and discussion related to the samarium oxide characterization (XRD and EDX) are presented in the [Supplementary Material \(SM\)](#).

### 2.1. Preparation of the catalyst

Initially, 2 g of  $\text{Fe}_2(\text{C}_2\text{O}_4)_3$  were mixed with 2 g of  $\text{NaBH}_4$  powder. The decomposition of the mixture was carried out in a horizontal tubular reactor. The reactor consisted of an alumina tube with inner diameter of 40 mm and length of 1000 mm. The synthesis was carried out with a heating rate of  $10\text{ }^\circ\text{C min}^{-1}$  from room temperature up to  $750\text{ }^\circ\text{C}$  in atmosphere. This temperature was kept for 2 h. After having completed this step, the reactor was cooled until room temperature.

### 2.2. Synthesis of boron nitride nanotubes

TCVD synthesis of BNNTs using boron (B)/catalyst powder (Catalyst/B = 0.02) and 1 wt% of samarium oxide was executed in a horizontal tubular reactor. The experimental apparatus is similar to the used by Ahmad and co-works (Ahmad et al., 2015). The reactor

consisted of an alumina tube with inner diameter of 40 mm and length of 1000 mm, with inlet and outlet for the flowing ammonia and nitrogen gas. Under atmosphere of  $\text{NH}_3/\text{N}_2$  mixture, the synthesis was carried out with a heating rate of  $10\text{ }^\circ\text{C min}^{-1}$  from room temperature up to  $1150\text{ }^\circ\text{C}$  and kept at this temperature for 1 h. After having completed this step, the reactor was cooled under atmosphere of  $\text{NH}_3/\text{N}_2$  mixture until room temperature.

### 2.3. Biological assay

#### 2.3.1. Cell culture

The MRC-5, a human lung fibroblast cell line (ATCC, VA, USA), was cultured at  $37\text{ }^\circ\text{C}$  in 5%  $\text{CO}_2$  in Dulbecco's modified Eagle's medium (Life Technologies, NY, USA) containing 10% fetal bovine serum (FBS), 1 mM sodium pyruvate, 50 units  $\text{mL}^{-1}$  penicillin, and  $100\text{ }\mu\text{g mL}^{-1}$  streptomycin (Life Technologies).

#### 2.3.2. Cell viability assay

The WST-8 assay was used to evaluate cell viability, which is based on the conversion of a water-soluble tetrazolium salt, 2-(2-methoxy-4-nitrophenyl)-3-(4-nitrophenyl)-5-(2,4-disulphophenyl)-2H-tetrazolium, monosodium salt, into a water-soluble formazan dye upon reduction by dehydrogenases in the presence of an electron carrier. Previously, MRC-5 cells ( $1 \times 10^4$ ) had been seeded onto a 96-well plate. After 24 h, it was verified whether cells were adhered to the plate surface. Then, the cells were incubated with 10, 50, 100 and  $200\text{ }\mu\text{g mL}^{-1}$  of as-grown and Sm-doped BNNTs. After 48 h, the extent of cell viability was assessed using a Cell Counting Kit-8 (CCK-8-Sigma-Aldrich). The CCK-8 solution ( $10\text{ }\mu\text{L}$ ) was added to each well, followed by incubation for 2 h at  $37\text{ }^\circ\text{C}$ . The absorbance at 450 nm was determined using a microplate reader (Multiskan GO; Thermo Scientific). All experiments were repeated three times with triplicate samples. Statistical analysis was performed by using Graph Pad Prism 5.0. The values were represented as the mean standard deviation. Statistical differences were calculated by using analysis of variance and Bonferroni's post-tests. Differences were considered significant at  $p < 0.05$ . Cell viability was expressed as a percentage relative to the untreated cells.

#### 2.3.3. Characterization

An ultima IV Rigaku Diffractometer with  $\text{Cu-K}\alpha$  radiation was employed to study the main crystalline phases in the synthesized materials. The Bragg angle values were varied in the range of  $20\text{--}90^\circ$  for the samples, with a scanning rate of  $0.02^\circ\text{ min}^{-1}$ . The data of the samples were compared with the program data Crystallographica Search-Match. FTIR measurements were performed with a Thermo Nicolet 6700 equipment. The spectra were collected in ATR mode with 64 accumulations in transmission mode and then systematically adjusted, taking baseline corrections into account. The SEM images were obtained using a Carl Zeiss Field Emission Scanning Electron Microscope, model sigma VP. Cathodoluminescent (CL) images were obtained with an accelerating voltage of 15 kV and aperture size of  $60\text{ }\mu\text{m}$ . The samples were dispersed in acetone for 30 min using an ultrasonic bath and one drop was placed onto a silicon substrate. The High Resolution Transmission Electron Microscopy (HRTEM) images and Selected Area Electron Diffraction (SAED) were obtained on a FEI TEM-LaB6 TECNAI G2 microscope with a tungsten filament electron gun of 200 kV. Electron energy loss spectroscopy (STEM-EELS) spectrum was obtained by a GIF Quantum SE detector system with energy resolution of 1.5 eV and dispersion of  $0.25\text{ eV/pixel}$ . The samples were dispersed in acetone for 30 min using an ultrasonic bath and one drop was placed onto a 200 mesh holey carbon copper grid. Energy dispersive X-Ray (EDX) measurements were performed with Shimadzu model EDX 720 equipment operating with target: rhodium anode, voltage: 50 kV, X-ray path: air, detector: silicon (lithium) and measurement time: 6 s. The measurement area was 1 cm in diameter. The radioisotope  $^{153}\text{Sm}$  was obtained by the irradiation of the Sm-doped BNNTs in the TRIGA Mark-1 of

Download English Version:

<https://daneshyari.com/en/article/8208787>

Download Persian Version:

<https://daneshyari.com/article/8208787>

[Daneshyari.com](https://daneshyari.com)